Numerical simulations of a storm-generated island-trapped wave event at the Hawaiian Islands

M. A. Merrifield, L. Yang, and D. S. Luther

Department of Oceanography, University of Hawaii at Manoa, Honolulu, Hawaii, USA

Received 9 September 2001; revised 4 April 2002; accepted 13 May 2002; published 24 October 2002.

[1] The structure and generation of subinertial trapped waves at the Hawaiian Islands are investigated using a primitive equation model with realistic bathymetry, stratification, and wind forcing. The strongest wave event measured on the island of Hawaii during the 1980s is selected as a case study. An extratropical cyclone traveling to the east provided the forcing. Three model runs are considered: a single island and a chain of islands forced by synoptic-scale winds and a chain of islands with enhanced winds to simulate features of the mesoscale forcing. Each model run documents the establishment of high and low surface elevation anomalies (0.05 m amplitudes) on opposite sides of the island of Hawaii due to convergences and divergences in the surface wind-driven current. Predicted along-shelf current amplitudes exceed 0.4 m/s, with the strongest currents near the surface and weak amplitudes (<0.1 m/s) below 100 m depth. Following the storm, a gravest mode island-trapped wave with a 59 hour period progresses around the island for at least five wave cycles. Although the storm itself lasts only 2 days, the rotation of the wind field in time reinforces the gravest mode wave at the island of Hawaii. A similar forced pattern is established at the other major islands; however, the free wave response is much weaker than at Hawaii because of a mismatch in the forcing and resonant wave mode frequencies. In comparison to tide gauge measurements and a current meter record from the northwest coast of Hawaii, the model shows similar time dependence, although amplitudes are underpredicted by approximately a factor of 2. Increasing the wind speeds near Hawaii yields closer agreement with the observations. Exchange of wave energy between the islands is weak (<10%) but noticeable, particularly in determining the decay rate of the Hawaii island-trapped wave. *INDEX TERMS:* 4512 Oceanography: Physical: Currents; 4255 Oceanography: General: Numerical modeling; 4544 Oceanography: Physical: Internal and inertial waves; 4219 Oceanography: General: Continental shelf processes; *KEYWORDS:* currents, coastal-trapped waves, numerical modeling, islands

Citation: Merrifield, M. A., L. Yang, and D. S. Luther, Numerical simulations of a storm-generated island-trapped wave event at the Hawaiian Islands, *J. Geophys. Res.*, *107*(C10), 3169, doi:10.1029/2001JC001134, 2002.

1. Introduction

[2] Coastal-trapped waves (CTWs) contribute significantly to the circulation along most continental shelves, particularly on timescales greater than the inertial period and less than typical weather systems (2–10 days). The along-shelf component of the surface wind stress is known to generate low mode CTWs that can propagate energy over considerable distances along the coast. In this way wind forcing along the coastal waveguide contributes both locally and remotely to coastal circulation over relatively broad time and space scales. The modal nature of CTWs is reflected in offshore structure and alongshore phase speed or wave number. A review of observational and theoretical studies of CTWs on continental shelves has been given by *Brink* [1991].

[3] An interesting variety of CTWs occurs on closed coastlines, such as around an island. Because the trapped wave energy is confined to a closed path, a resonance can exist whereby waves with an integer number of wavelengths, or continuous phase, around the island are reinforced. In contrast to CTWs, the energetic timescales for island-trapped waves, or ITWs, are associated with wavelengths that approach this azimuthal phase continuity. How effective winds are in generating or sustaining ITWs will depend largely on the direction and amplitude of the forcing relative to the phase of the wave as it progresses around the island.

[4] *Longuet-Higgins* [1969] provided a theoretical context for subinertial ITWs by examining wave trapping about a cylindrical island in a homogeneous, rotating fluid. The theory was extended to include stratification by *Wunsch* [1972]. Following *Wunsch* [1972], free ITW modes are specified according to their azimuthal (n) and radial (m) mode number. In terms of baroclinic pressure, the modal expansion can be expressed as

$$p(r,\theta,z) = \sum_m \sum_n u_m(z) K_n(k_m r) e^{-i(n\theta+\omega t)}$$

0148-0227/02/2001JC001134$09.00

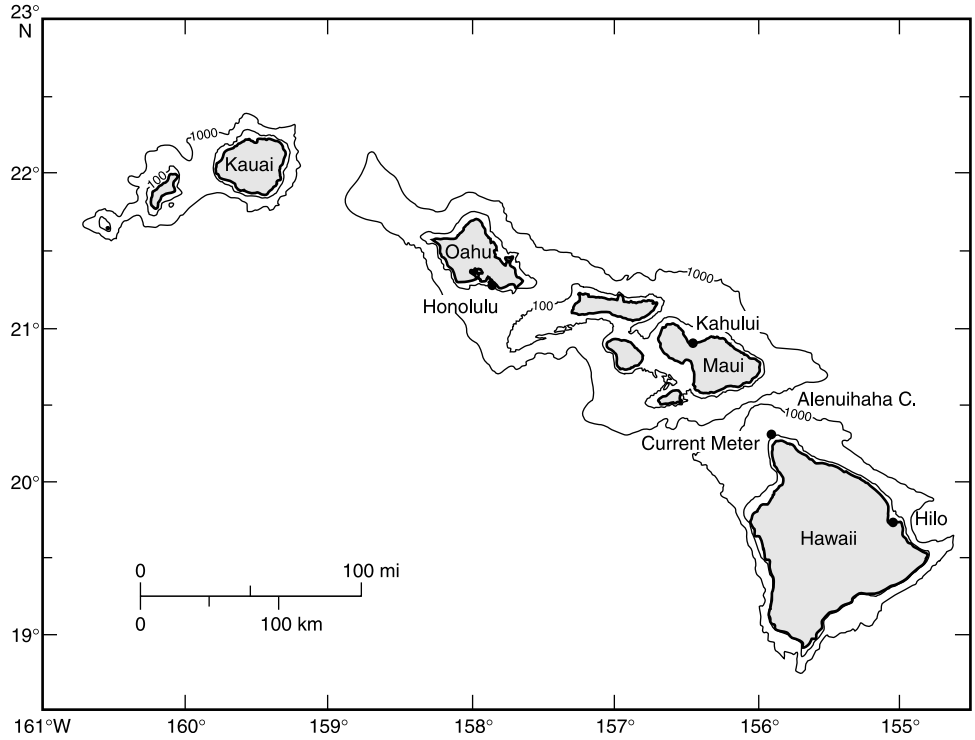

Figure 1. The main Hawaiian Islands with the locations of the observations used in this study. The 100 and 1000 m isobaths are included. The Maui island group refers to the four islands lying within the 100 m isobath near Maui. Note the largest island in the Hawaiian Islands is called Hawaii.

with the horizontal wave number for mode m given by

$$k_m^2 = \left(1 - \omega^2/f^2\right)\lambda_m^2,$$

and the vertical structure for mode m satisfying

$$\frac{\partial}{\partial z}\left[\frac{f^2 u_m'(z)}{N^2(z)}\right] = -\lambda_m^2 u_m(z)$$

with the boundary conditions $\partial u_m/\partial z = 0$ at the surface and bottom, and no normal flow at the sides of the island ($r = a$). $K_n(k_m r)$ is a modified Bessel function, ω is the wave frequency, f is the Coriolis parameter, λ_m is the Rossby deformation radius, N is the buoyancy frequency, and r, θ, z are the radial, azimuthal, and depth coordinates. The gravest ITW mode corresponds to m, $n = 1$ with one wavelength around the island and one zero crossing in the offshore structure. The influence of sloping topography on ITW modes has been treated by *Brink* [1999].

[5] Observational evidence for ITWs has relied largely on the detection of energetic peaks in coastal sea level and temperature spectra that correspond to theoretical wave modes (*Munk and Cartwright* [1966], *Miyata and Groves* [1968, 1971], and *Longuet-Higgins* [1971] for Oahu, Hawaii, and *Wunsch* [1972] for Bermuda]. The first extensive description of ITWs using moored observations was made by *Hogg* [1980] for Bermuda. Comparisons of spectral estimates with predicted wave modes based on *Wunsch* [1972] suggest the presence of subinertial baroclinic waves with modes one and two azimuthal and modes one through four radial structure. The ITWs appear to be forced by local surface winds. Hogg identified a 26.1 hour peak in current and temperature spectra, Bermuda's gravest subinertial ITW mode, and found that energy in this band was coherent with surface wind stress in a manner indicative of resonant forcing. The Bermuda ITWs are more energetic during the winter than summer months. Frictional dissipation appears to be weak as Hogg found a Q of 20. Q, the ratio of center frequency to peak half width, provides an approximate measure of the number of wave cycles that will occur in the presence of dissipation [*Munk and MacDonald*, 1960].

[6] *Luther* [1985] did a thorough study of Hawaiian Island sea level spectra from tide gauges located at Kauai, Oahu, Hawaii, and the Maui island group (Figure 1), relating observed peaks and phase differences with computed ITW mode frequencies. Two tide gauge records on Oahu indicate ITW peaks at 34.5 and 47 hours, corresponding to the mode-one azimuthal/mode-one radial wave, and the mode-one azimuthal/mode-two radial wave, respectively. The most energetic signal was observed at Hilo on the island of Hawaii with RMS sea level amplitudes on the order of 1 cm. A spectral peak at 59 hours corresponds to the gravest mode for this, the largest of the Hawaii Islands. The spectral bandwidth corresponds to a Q of aproximately 7. The theory of *Wunsch* [1972] suggests corresponding alongshelf current speeds of less than 5 cm/s. Although the offshore structure of the waves was not measured, Luther noted that the strong stratification and steep island slopes of the Hawaiian Islands are consistent with internal Kelvin wave dynamics. An energetic peak was also found at

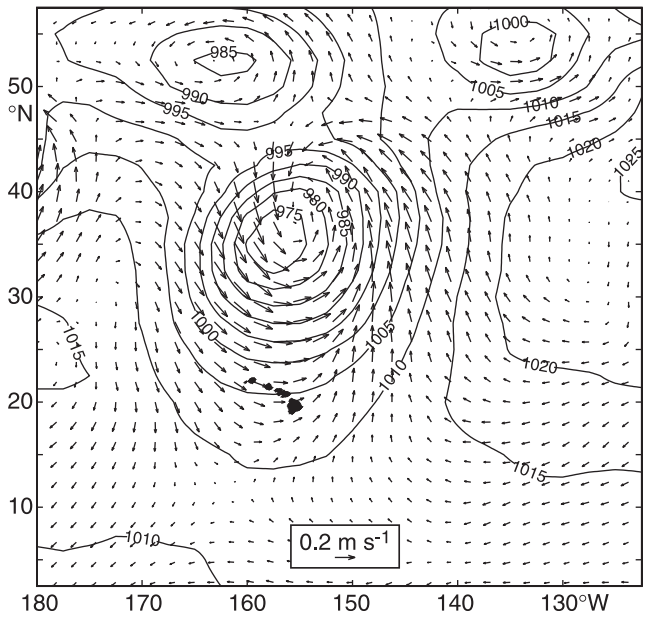

Figure 2. Surface winds and pressure for 18:00 Z 14 January 1985 from the National Center for Environmental Prediction (NCEP) Reanalysis Model.

Kahului Harbor on the island of Maui at a period of 64 hours and a Q of 8.5. Luther noted that the islands of Maui, Molokai, Lanai and Kahoolawe are separated by shallow channels and appear to be a single island below the base of the thermocline. The 64 hour peak likely indicates trapping around the entire island group rather than around Maui itself. As in the case of Bermuda, the ITW energy levels are higher in the winter months but appear as more isolated events than the Bermuda record. Luther also proposed that the trapped wave at the Maui group of islands may be forced by leakage from the energetic wave trapped to the island of Hawaii.

[7] *Lumpkin* [1995] examined the subinertial oscillations at the Hawaiian Islands described by *Luther* [1985] and developed a simple model to consider a flat-topped, cylindrical island with an imposed homogeneous, unidirectional, oscillating wind stress. Correspondences between theoretical eigenfrequencies obtained from the model and observed spectral peaks in sea level and current records provide evidence for the wind forcing of low mode subinertial ITWs. Lumpkin further concluded that remote forcing may play a role in generating some of the variance of the trapped wave at Hilo, but that leakage from Hawaii to the Maui group seems to be the dominant forcing mechanism for the spectral peak observed at Kahului.

[8] In short, the observational studies to date have largely confirmed the presence of resonant azimuthal ITW modes around various islands by the identification of spectral peaks and azimuthal phase relationships that correspond well with theoretical predictions based on idealized cylindrical topographies [*Wunsch*, 1972]. Cross-spectral estimates point to wind forcing as the primary generation mechanism, which is consistent with the model results of *Lumpkin* [1995]. For closely spaced islands such as the Hawaiian chain, interisland ITW energy transfer has been proposed.

[9] Here we examine the structure and generation of subinertial ITWs at the Hawaiian Islands with numerical simulations using the Princeton Ocean Model (POM). To our knowledge this is the first modeling study of ITWs that uses realistic bathymetry, stratification, and wind forcing. Given the event-like nature of the ITWs at Hawaii [*Luther*, 1985], we focus on a case study of a winter storm that passed over the islands from 13–15 January 1985 (Figure 2). National Center for Environmental Prediction (NCEP) reanalysis winds, which are used to force the model, reached open ocean speeds of 12 m/s near Hawaii during the storm, with winds rotating anticyclonically from northward at the start of the storm to southward at the conclusion as this intense extratropical cyclone moved to the east (Figure 3). The ITW sea level response associated with this storm was the largest amplitude event observed at Hilo during the 1980s (0.2 m peak to trough, Figure 3). The event was captured in current meter observations off the coast of Hawaii in the Alenuihaha Channel (Figure 1). Observed alongshelf currents associated with this storm, measured 20 m below the surface in 169 m total depth, exceeded 0.5 m/s in amplitude with a well-defined mode-one periodicity (Figure 3).

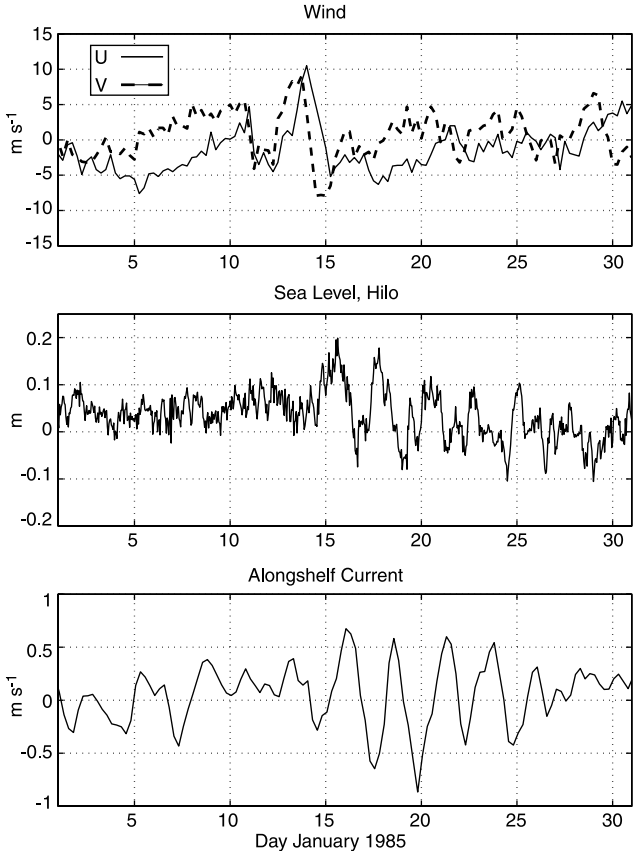

Figure 3. Time series of 6 hourly NCEP reanalysis winds (U, east–west component and V, north–south component), hourly tide gauge data from Hilo Harbor on the island of Hawaii (detided), and the along-shelf current measured 20 m below the surface in 169 m water depth in the Alenuihaha Channel (detided and smoothed with a 12 hour running mean filter).

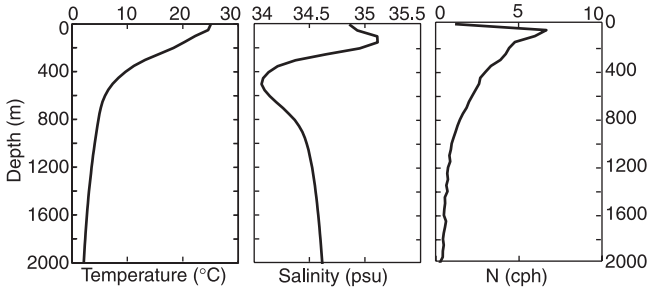

Figure 4. Temperature, salinity, and buoyancy frequency profiles used in the model. The temperature and salinity profiles are annual means for the region from *Levitus* [1994] World Ocean Atlas data.

[10] Three different model runs are examined: a single island run for the island of Hawaii, an island chain run spanning the islands of Hawaii to Oahu, and an island chain run in which the wind forcing is augmented to take into account orographic effects around tall volcanic peaks. Our focus is on the island of Hawaii and the Maui group of islands because the dominant ITWs at these sites are well separated in frequency from inertial motions that also arise in response to the variable wind forcing. Inertial and resonant ITW motions are more difficult to separate at Oahu and Kauai in short duration model runs.

[11] The layout of the paper is as follows. The numerical model and model grids are described in section 2. Model results for the Hawaii island run are presented and compared to the observed current and sea level records (3). While the overall character of the lowest mode ITW appears to be captured in this run, there are discrepancies between the observed period and wave amplitude. The wind-forced response of the island chain is then considered (4). The modeled ITW period for the mode-one Hawaii island ITW is in better agreement with observations than the single island run, which we attribute to the influence of the nearby islands on the Ekman transport. A mode-one response is also found at the Maui island group, although direct wind forcing rather than leakage from the island of Hawaii appears to be the primary energy source. Observed ITW amplitudes at Hawaii are still underpredicted in these runs forced by synoptic-scale winds. To determine whether orographic effects might improve the comparison with observations, we force the island chain run with a locally modified wind field that is intended to model accelerations around high volcanic peaks (5). Model ITW amplitudes are more realistic than in the previous runs as a result. A summary and concluding remarks are given in the final section.

2. Model Description

[12] We use the Princeton Ocean Model, a fully three-dimensional, nonlinear, free surface, hydrostatic, sigma coordinate, primitive equation model that incorporates a Mellor Yamada level 2.5 turbulence closure scheme. A detailed description of POM is given by *Blumberg and Mellor* [1987]. A similar configuration of POM also has been used for the Hawaii region to study internal tide generation [*Merrifield et al.*, 2001]. The model is run with a constant Coriolis parameter corresponding to an inertial period of 35.9 hours. The model stratification is defined from annual average temperatures and salinities for the region (Figure 4). The prognostic variables used in this study are the sea surface elevation, the horizontal current, and temperature.

[13] A radiation condition on the barotropic and baroclinic velocity component normal to the boundary is applied on the east and west open boundaries. The tangential velocities are set to zero on both boundaries. On the north and south boundaries, a wall boundary condition is used. The wall condition was found to stabilize the model during the testing phase when various wind forcings were specified. Although open boundaries may have served our purpose as well in the final model simulations, the closed north–south boundaries were maintained since the effects of the wall did not influence noticeably the model results in the vicinity of the islands.

[14] Two model grids are used for this study. In both cases model bathymetry is specified using standard interpolations from the Smith-Sandwell topography [*Smith and Sandwell*, 1997]. The first model grid is for the island of Hawaii (here we refer to the island itself as Hawaii and the chain as the Hawaiian Islands) (Figure 5a). The single island runs are conducted in a square domain (739 km $\times$ 739 km) with a variable grid spacing ranging from 10 km near the boundaries to 3 km near the island. Realistic bathymetry is used for the island; however, the deep ocean is set to a constant depth of 4500 m. The bathymetry of the island chain separating Hawaii from Maui also is augmented in this run to ensure a smooth transition to the ocean floor. For the island chain runs, realistic bathmetry is used from the island of Oahu to the northwest to Hawaii at the southeast (Figure 5b). The island of Kauai was excluded in these runs because of the computational overhead required in extending the grid to this outer island. The computational domain was 524 km $\times$ 572 km with a uniform grid spacing of 4 km.

[15] In all runs, 16 sigma levels are used in the vertical, evenly spaced except for the top nine points that are logarithmically spaced to improve resolution in the surface Ekman layer. Test runs using 21 and 51 sigma levels produced results that were nearly identical to the16 level runs in terms of the comparisons to the observations and in the overall ITW fields depicted. The coarser vertical resolution grid is used to allow for larger lateral domains. The horizontal diffusion is parameterized using the Smagorinsky

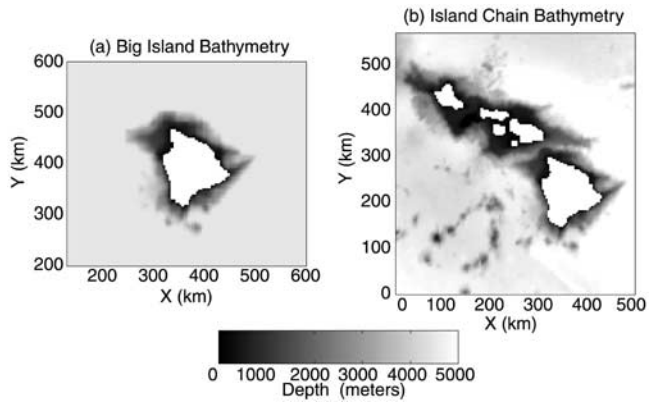

Figure 5. The bathymetry used in the (a) single island and (b) island chain model runs.

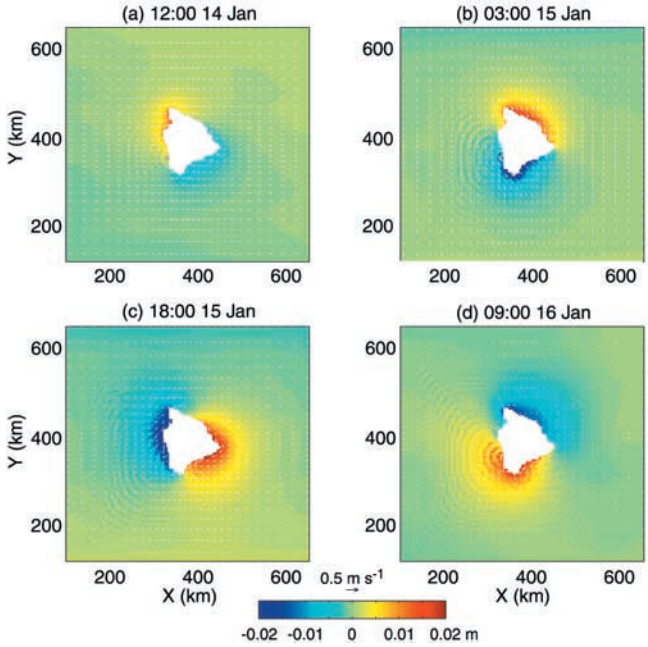

Figure 6. Model results from the single island run showing the surface elevation (color contour) and current (vectors) (a)–(c) during and (d) after the storm. The mode-one azimuthal wave propagates anticyclonically around the island.

diffusivity (see *Kantha and Clayson* [2000] for a description). Test runs using 0.0, 0.1, and 0.2 for the Smagorinsky coefficient all yield similar results. The coefficient was set to 0.1 for all model runs.

[16] Numerical errors resulting in artificial flows can occur when using sigma coordinate grids over steep bathymetric slopes [*Mellor et al.*, 1994]. We evaluated this error by running the model with zero wind forcing. Although the resulting flow speeds are generally weak (order 0.0001 m/s), a few areas around the steep slopes of Hawaii develop large amplitude drift (0.1 m/s) over the course of the model simulation. RMS amplitudes in the ITW frequency bands of interest, however, are an order of magnitude weaker than the ITW signals. We conclude that numerical errors of this kind do not affect our interpretation of the ITW signal.

[17] The model is forced using NCEP 6 hourly surface winds for the time period 12–30 January, 1985 (Figure 3). A one day ramp from zero wind forcing is used at the beginning of the run. At the spatial resolution of the NCEP winds ($\sim$1.9°), the wind field is fairly uniform in the vicinity of the Hawaiian Islands. Therefore in the model runs reported in sections 5 and 6, a spatially uniform wind forcing was applied over the computational domain. Model tests using spatially varying winds were nearly identical to the uniform wind-forcing runs. In section 7, we attempt to model the orographic acceleration of the wind field around Hawaii where summit peaks exceed 4 km in height.

3. Results for a Single Island

[18] Our first model run using the Hawaii island grid illustrates the general structure of the trapped wave associated with the mid-January storm event. As the storm approaches on14 January, maximum northward winds cause surface Ekman transport to the east and a sea level convergence/divergence on the northwest/southeast sections of the island (Figure 6a). When the low pressure system is centered to the north (Figure 6b), strong eastward winds change the course of the Ekman transport in the open ocean toward the south with a corresponding shift in the sea level anomaly pattern to the north and south shores. As the storm passes to the east (Figure 6c), strong southward winds further enhance the trapped wave signal. On January 16 as the winds subside (Figure 6d), a freely propagating ITW remains with one azimuthal cycle about the island. Enhanced coastal currents associated with the ITW are evident at the island whereas directly forced deep ocean current speeds have diminished with the passage of the storm. The short wavelength patterns in Figures 6b–6d (also later in Figure 10 are associated with numerical noise in the simulations. We do not believe that this noise affects our interpretations of the model results in the ITW frequency bands of interest.

[19] The period of the ITW is approximately 58.7 hours in the model simulations, similar to the period of the gravest mode ITW predicted by *Luther* [1985] for Hawaii (59.5 hours). RMS amplitudes are estimated in the frequency band 0.32–0.55 cpd (periods 43.8–74.4 hours) for sea surface elevation and surface current. This band excludes inertial variability. Both fields clearly illustrate the trapping of energy at the island (Figure 7). An approximate *e*-folding scale for the elevation field is 45 km, comparable to the first baroclinic Rossby radius of 65 km computed for the stratification depicted in Figure 4. Although the model time series is too short for a careful spectral decomposition, enhanced energy around the island was not evident at 102.5 hours, which corresponds to the theoretical period for a mode-two azimuthal, mode-one radial wave for Hawaii [*Luther*, 1985]. Another theoretical mode at these timescales is the mode-two azimuthal and radial wave (52.5 hours). There is little indication in the model, however, for mode-two azimuthal structure in the trapped energy. It appears that the gravest wave mode is the primary response to the storm, which is consistent with this being the most energetic ITW mode observed in Hilo sea level as well as the most energetic ITW signal observed at any of the other Hawaiian Island tide gauge stations [*Luther*, 1985].

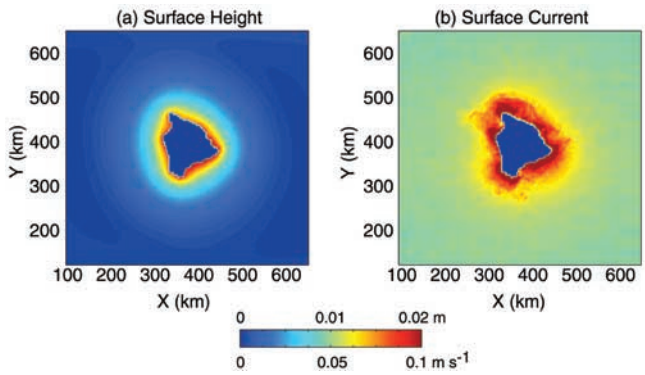

Figure 7. The RMS surface elevation and current speed in the frequency band 0.32–0.55 cpd (periods 43.8–74.4 hours) for the single island run.

[20] A comparison of model and observed Hilo sea level and Alenuihaha along-shelf current shows discrepancies in both amplitude and phase (Figure 8). The initial directly forced model sea level crest at Hilo at the onset of the storm resembles the observed peak, although the amplitude is underpredicted by 0.01–0.02 m. As the trough passes Hilo on 16 January, the amplitude discrepancy is closer to 0.04 m and the model wave begins to lead the observations. By the second wave crest, the model leads the observed wave in time by nearly 6 hours and remains so for at least four more wave cycles. The discrepancy in timing is due primarily to a time delay as opposed to a difference in wave period. Following the storm, the observed and model wave periods are close to 59 hours. Similar results hold for the model and observed along-shelf current comparison, although the modeled current is weaker than observed by nearly a factor of 2 during the period of direct storm forcing (14–15 January).

[21] The decay of the wave signal in time after the storm passage also differs between the model and observations. The wave lasts 5–6 cycles in the observed alongshelf current record, and perhaps 1 or 2 cycles more in Hilo sea level (Figures 3 and 8). In contrast, after 5–6 cycles the model sea level and current amplitudes are nearly 50% of initial values. The model simulation for the isolated island therefore underestimates the observed dissipation of the wave signal.

[22] Although questions remain regarding the predicted timing, amplitude, and decay of the wave event, the general azimuthal (mode-one) and offshore structure of the wave in this model run is representative of all the runs that we considered. Currents are directed along isobaths with maximum amplitudes at the surface between 5 and 10 km from shore (Figure 9). During the passage of the first wave crest at the south end of the island (Figure 6d), alongshelf currents are westward over most of the water column down to 250 m depth. The surface flow is balanced by weaker eastward flows at deeper depths with speeds less than 0.1 m/s. The temperature field shows a coastal downwelling coinciding with the crest in surface elevation. Vertical displacements of 100 m occur at the coast with amplitudes decaying within 50 km. The offshore structure resembles a mode-one internal Kelvin wave, which is consistent with the strong stratification and steep topographic slopes encountered (0.13 at this site) and the absence of a well-defined shelf area (Figure 9). As anticipated from the results of *Luther* [1985] and *Lumpkin* [1995], the model simulation indicates that the dominant trapped response at Hawaii has mode-one radial as well as azimuthal structure.

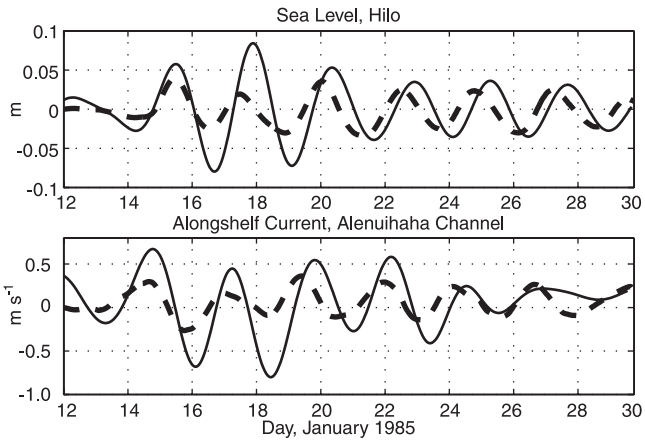

Figure 8. Comparison of observed (solid) and model (dashed) sea level (a) at Hilo and (b) alongshelf current in the Alenuihaha Channel for the single island run. The observations have been band-passed filtered (0.32–0.55 cpd).

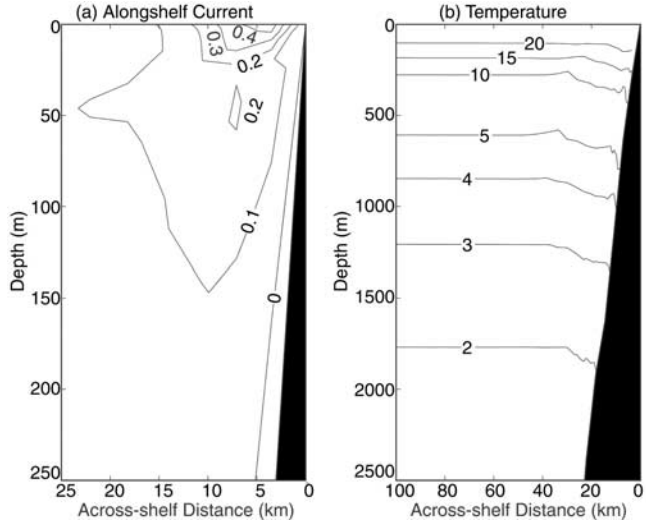

Figure 9. Offshore profiles of model (a) along-shelf current and (b) temperature for 09:00 Z 16 January 1985. The transect is located at the southern end of the island of Hawaii at model coordinate x = 357 (Figure 6).

4. Results for the Island Chain

[23] Our next model simulation includes the main Hawaiian Islands from Hawaii to Oahu. The purpose of this run is to examine the wind-forced response around the other islands and to determine whether realistic bathymetry linking Hawaii to the Maui group influences the Hawaii ITW signal. Using the same wind forcing as in the previous single island run, we obtain similar results. The storm winds generate high and low surface elevations on opposite sides of Oahu and Hawaii and around the Maui group of islands (Figure 10). As suggested by *Luther* [1985], the relatively shallow water within the Maui island group results in the dominance of a single mode-one azimuthal pattern around the entire group rather than around each individual island. During the time of direct wind forcing (Figures 10a–10c), the sea level highs and lows progress around Oahu, Hawaii, and the Maui group in phase with the rotating winds.

[24] The RMS amplitude of the surface elevation in the frequency band 0.32–0.71 cpd (periods 33.8–74.4 hours) is significantly higher around Hawaii than the other islands (Figure 11a). The next most energetic region in terms of surface elevation is the Maui group. We note that the RMS elevation in the center of this island cluster is near zero, indicating again that the energy propagates around the cluster rather than around each individual island. For this particular event, the trapped energy at Maui is generated primarily by the local wind forcing rather than an energy transfer from Hawaii. The weakest signal is at Oahu. This frequency band includes the gravest mode ITW at Oahu (35 hours) [*Luther*, 1985] and also near-inertial motions (inertial

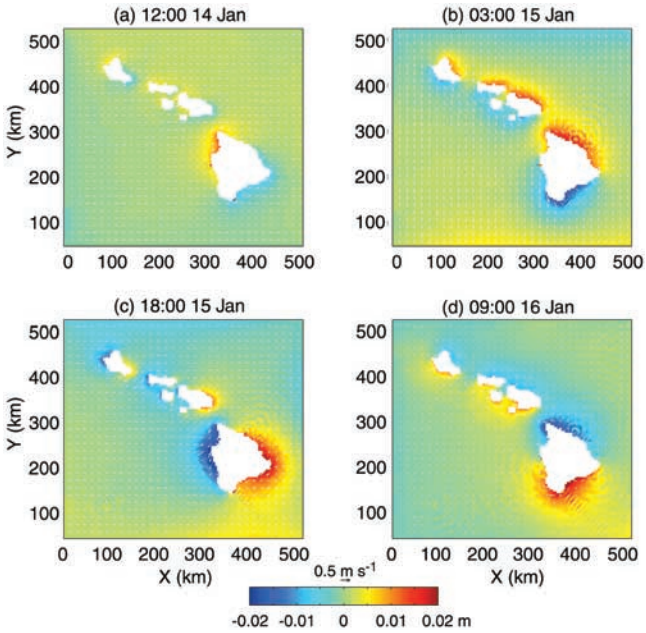

Figure 10. Model results from the island chain run showing the surface elevation (color contour) and current (vectors) (a)–(c) during and (d) after the storm. The mode-one azimuthal wave propagates anticyclonically around the islands.

period = 35.9 hours). Although a forced response similar to Hawaii is established at Oahu (Figure 10a), it apparently is unable to sustain itself as a free wave. The current amplitudes are enhanced around all the islands, consistent with trapped wave signals (Figure 11b). The open ocean current ampitudes are larger in the island chain run (Figure 11b) compared to the single island run (Figure 7b) because the band-pass filter in the latter removes inertial variability.

[25] We do not examine the resonant ITW period band at Oahu in this study because of competition with near-inertial motions at these timescales. Model tests with wind forcing near the inertial period indicate enhanced surface elevations and diminished current amplitudes near the islands due to a blocking effect of the open ocean inertial current field by the island topography. The inertial band sea surface amplitudes at the island coast are comparable to those of a resonant ITW at Oahu, making it difficult to separate the two processes using sea level alone.

[26] At Hawaii, the model and observed ITW signal at Hilo and at the Alenuihaha Channel (Figure 12) are more closely aligned in time than in the single island run (Figure 8). This timing difference between the two runs is not due to a change in phase speed caused either by the inclusion of the channel or realistic deep ocean bathymetry (the single island run used a constant depth open ocean). A phase speed change would result in a shift in the dominant period of the wave, which is not apparent in the single island and island chain runs as both are close to 59 hours. The time shift in the single island run relative to the observations seems to occur soon after the wind forcing subsides as the first wave trough passes Hilo (Figure 8). The shift then corresponds to a time delay of the wave in the island chain run between Figures 10c and 10d, when the wave trough at Hawaii encounters the wave crest moving around the Maui group. It appears that at the onset of

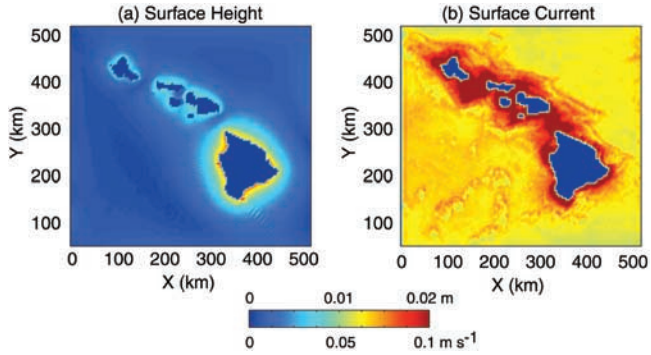

Figure 11. The RMS surface elevation and current speed in the frequency band 0.32–0.71 cpd (periods 33.8–74.4 hours) for the island chain run.

the storm when both waves are large, this interaction may cause a slight decrease in the Hawaii wave phase speed due to advection or some interaction with the adjacent wave crest. This is consistent with the time shift occurring only early in the event and not later when the waves are weaker and less likely to interfere with one another.

[27] The model continues to underpredict the observed amplitudes in both sea level and currents (Figure 12). The

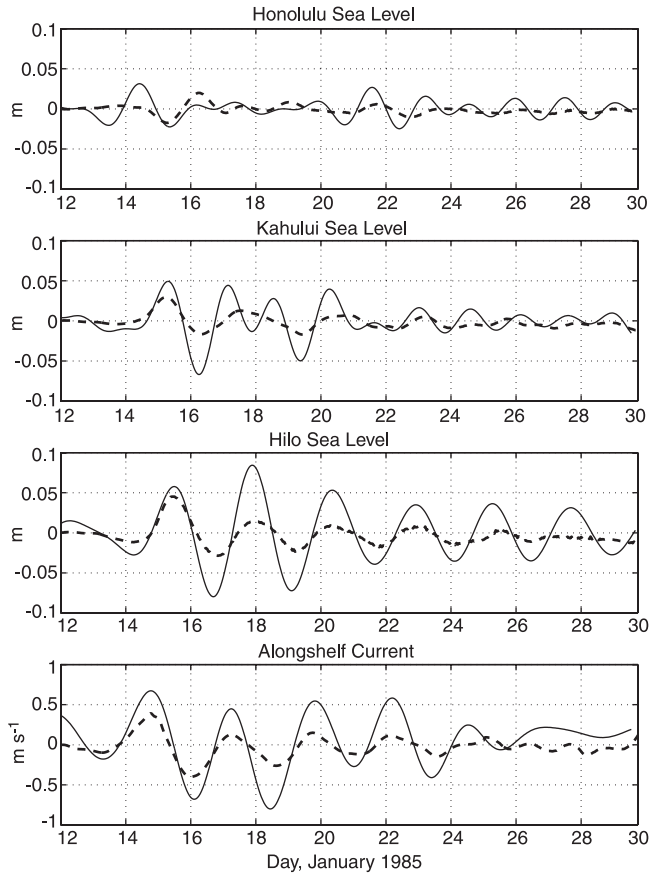

Figure 12. Comparison of observed (solid) and model (dashed) sea level at Honolulu, Kahului, and Hilo and along-shelf current in the Alenuihaha Channel for the island chain run. The observations have been band-passed filtered (0.32–0.71 cpd).

peak to trough amplitudes of the model sea level and along-shelf current are approximately one third of the observed values.

[28] Compared to the single island run, the island chain run displays a faster wave decay with the event lasting approximately five cycles, similar to the observed decay. Two possible explanations for the faster decay in the island chain run are increased bottom friction due to the realistic Alenuihaha Channel bathymetry, or energy leakage to the Maui island group as suggested by *Luther* [1985]. To estimate the influence of bottom friction, we decreased the bottom stress term in the island chain run by a factor of 10. This had little effect on the model decay time, suggesting that bottom drag is not a first order effect in terms of wave dissipation. The issue of energy transfer between islands will be addressed in section 5.

[29] The model sea level time series at Honolulu and Kahului show a weak (0.02–0.03 m) forced response during the storm that persists for only one to three cycles following the storm (Figure 12). At Honolulu, the forced response does not correspond to a theoretical ITW with mode-one azimuthal structure and hence a resonant free wave does not evolve. The model and observed sea level at Honolulu are not in agreement, except in that they are both weak during this period. At Kahului, the model and observed ITW signal are in better agreement than at Honolulu, although there are short period oscillations apparent in the observed record that mask the longer timescale oscillations predicted by the model. The wave period following the storm is approximately 72 hours at Kahului, longer than the Hawaii wave and similar to the theoretical prediction of *Luther* [1985] for the gravest mode period of 67 hours around an equivalent cylindrical topography.

5. Wind-Forcing Considerations

[30] The major discrepancy between the model and observed time series is the wave amplitude. We caution at the start that the comparisons are between point field measurements and model results obtained with 3 to 4 km horizontal resolution. The model also does not resolve regions of the coast shallower than 50 m where the coastal tide gauge stations are located. Given these caveats, we consider the influence of the wind forcing on model energy levels. We have treated the wind field as spatially uniform in the model runs considered so far. Anecdotal evidence suggests that the NCEP model may not capture the high wind speeds associated with this intense extratropical cyclone. The wind and wave damage caused by the storm made front page headlines in local newspapers, with surf reported up to 25 feet and widespread power outages due to high winds. Moreover, ship reports of 20 m/s were made in the region.

[31] A second consideration is orographic influence on the airflow, particularly near Hawaii and Maui where volcanic summits reach 4.1 km compared to 1–2 km on the lower western islands. *Wang et al.* [1998] has simulated various mesoscale features around the Hawaiian Islands, including airflow deceleration upstream and downstream of mountains, and acceleration around mountain flanks. The neglect of orographic effects would result in an under-prediction of coastal wind speeds.

[32] We examine the effect of enhanced winds around the Hawaii topography by arbitrarily doubling the NCEP wind speeds in the vicinity of the island. The affected region corresponds to the dark area in Figure 5a. We do not modify the winds at the other islands, in part because orographic effects have been shown to be weaker than on Hawaii [*Wang et al.*, 1998], and to determine whether enhanced energy around Hawaii leaks to the other islands, particularly the Maui group as suggested by *Luther* [1985] and *Lumpkin* [1995]. The simulation results in better agreement with observed sea level and current amplitudes at Hawaii than achieved in the previous model runs (Figure 13 compared to Figures 8 and 12). In particular, the along-shelf current time series agree quite well for the duration of the event. The model and observed Hilo sea level are similar during the storm (first wave crest), but the model sea level remains weaker by nearly a factor of 2 following the storm.

[33] The model response at the Maui and Honolulu tide gauges due to enhanced winds at Hawaii is nearly unchanged from the previous island chain run suggesting weak ITW energy transfer from Hawaii to the other islands across the Alenuihaha Channel (Figures 12 and 13). The depth-integrated kinetic energy for the two model runs, however, does indicate energy exchange. The energy is obtained by fitting a 59 hour harmonic to the horizontal currents for the time span 14–23 January. The energy is averaged over a wave period. Figure 14 shows the ratio of kinetic energies obtained from the enhanced wind run and the original island chain run. The enhanced winds around the island of Hawaii result in a factor of 2–3 increase in kinetic energy. Although the wind speeds over the remaining islands are identical for the two runs, there is a noticable increase in energy around the Maui group and Oahu of 1.5–2 in some locations. The energy amplification shown in Figure 14 tends to be stronger on the western side of the Maui group than the east, consistent with ITW energy originating from the Alenuihaha Channel and decaying as it propagates anti-cyclonically around the adjacent islands.

[34] Returning to the comparison of the island chain run (Figure 12) and the single island run (Figure 8), it was noted that the wave signal appears to decay more quickly in the former than the latter. We now attribute this difference to energy leakage from the gravest mode ITW at Hawaii to the neighboring islands. An approximate estimate of the average (from 14 to 23 January) ITW energy around the entire island of Hawaii in the island chain run is 10^{13} Joules (J). The northward flux of energy past the across-shelf transect pictured in Figure 14 at the Maui group is on the order of 10^{12} J over one wave period. Thus, about one tenth of the total wave energy at the island of Hawaii is transported northward near the Maui group. On the eastern side of Maui, the energy fluxes are at least an order of magnitude smaller than on the west. If the energy were solely due to a near resonant ITW around the Maui group, we would expect more constant energy flux levels on either side of the island group. Instead we attribute much of the northward energy flux (at the 59 hour period) on the western flank of the Maui group to energy that orignates from the island of Hawaii. The energy is contained in a nonresonant frequency band for the Maui group; hence it decays to negligible energy flux levels on the eastern side. This would include Kahului Harbor where the ITW signal did not change much between

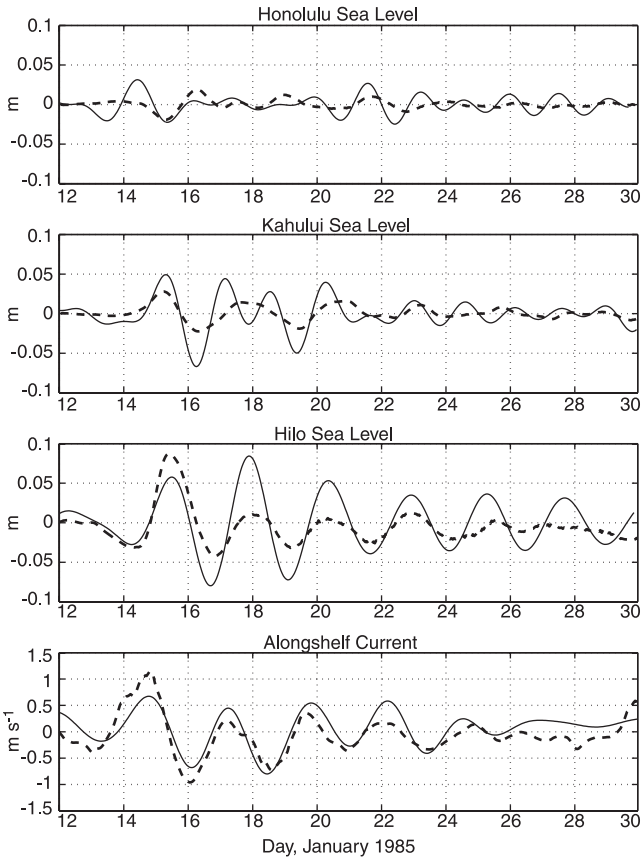

Figure 13. Same as Figure 12 but for the case of enhanced wind forcing around the island of Hawaii.

the orignal and enhanced wind model runs. An upper bound estimate of the energy loss of approximately 10% with each gravest wave mode circuit around the island of Hawaii would result in a factor of 2 reduction in total energy after five wave periods, which is consistent with the enhanced decay found in Figure 12 compared to Figure 8.

6. Summary

[35] We have examined an energetic ITW event at the Hawaiian Islands associated with the passage of a winter storm. The storm winds drive a surface Ekman current that results in sea level convergences and divergences around the major islands. Although the storm itself is short-lived (2–3 days), a large amplitude trapped wave is established at the island of Hawaii corresponding in period to the gravest mode ITW. This particular storm is effective at generating the gravest mode wave at Hawaii because the anticyclonic rotation of the winds in time serves to reinforce this particular wave mode around the island. Similar features are established around the Maui Island group and Oahu, although weaker in amplitude and shorter-lived in duration than on Hawaii. Apparently the forced response established by the storm winds does not correspond as well with resonant ITW modes at these other island sites compared to Hawaii. In addition, the Maui group may not be as effective a coastal barrier as Hawaii, leading to a weaker wave signal.

[36] The model results are compared to tide gauge measurements at Hilo, Kahului, and Honolulu, as well as alongshelf coastal currents measured just off the northwest tip of Hawaii in the Alenuihaha Channel. The first model run considers Hawaii in isolation with synoptic scale wind forcing (i.e., spatially uniform winds). The model underestimates the observed amplitudes by at least a factor of 2 and leads the observed wave signal by nearly 6 hours once the storm subsides. The decay of the wave is also slower in time for the model than observed.

[37] A second run considers the island chain bathymetry from Oahu to Hawaii with the same wind forcing as in the first run. The timing of the model ITW agrees more closely with the observations than in the single island run, which we attribute to the presence of the channel. The major time shift occurs shortly after the subsidence of the storm, suggesting that only higher amplitude waves that span the channel actually experience this delay. Weaker waves presumably do not interact with the trapped waves or bathymetry of the adjacent island. Although the timing is in better agreement with observations than the single island run, the amplitude remains weaker than the observed signal by a factor of 2.

[38] In the last simulation, we examine the effect of stronger winds near Hawaii by doubling the coastal wind speeds during the storm passage. The wind field over the remaining islands is not altered. The result is that model amplitudes are in closer agreement with the observations than in the previous runs. By limiting the wind enhancement to Hawaii, we also find that leakage of energy from Hawaii to adjacent islands does occur. For this particular storm, on the order of 10% wave energy loss from the Hawaii ITW to the Maui group is found.

[39] We have examined only one storm of rather unusual strength, which raises the issue of how representative this

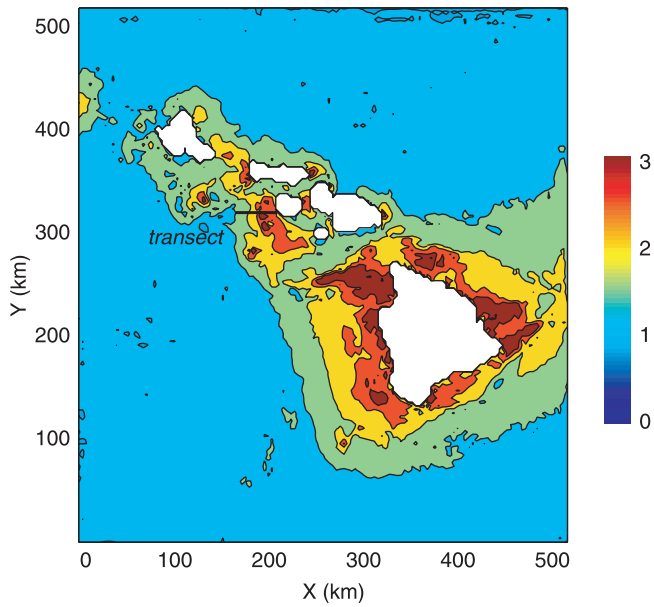

Figure 14. The ratio of depth-averaged kinetic energies obtained from the model run with enhanced winds around the island of Hawaii and the original island chain run. A value greater/less than one indicates more/less energy in the enhanced wind run.

event is of others that generate ITWs at the Hawaiian Islands. A more comprehensive study of ITWs in this region will follow using new data sources. The results of our study will then be compared and contrasted with other ITW events. We believe that the basic generation mechanism and overall structure of gravest mode ITWs at Hawaii have been addressed in this work, and that interisland energy transfer is probably not a major issue, but may explain the smaller Q ($\sim$7, indicating higher dissipation) estimated by *Luther* [1985] for Hawaii ITWs than by *Hogg* [1980] (Q $\sim$ 20) for Bermuda ITWs. Recommendations for future modeling studies of this type include higher grid resolution near the coast particularly where field observations are available for comparison, improved wind-forcing fields that include mesoscale variations, and consideration of the forcing conditions condusive for higher ITW mode generation.

[40] **Acknowledgments.** This work was supported by the National Science Foundation (OCE-9522092). M. Merrifield also received support from the Office of Global Programs, NOAA (NA67RJ0154). Discussions with K. Brink, P. Holloway, S. Johnston, and F. Davidson are greatly appreciated. S. Nakahara assisted with the data preparation. NCEP Reanalysis data and NODC World Ocean Atlas 1994 [*Levitus*, 1994] data were obtained from the NOAA-CIRES Climate Diagnostics Center, Boulder, Colorado, USA (http://www.cdc.noaa.gov/). Tide gauge data were obtained from the University of Hawaii Sea Level Center (http://uhslc.soest.hawaii.edu/). The current meter observations were made by Noda and Associates, Honolulu, Hawaii, and the data were obtained from P. Caldwell, the NOAA/NODC/NCDDC Regional Liaison Officer at the University of Hawaii.

References

Blumberg, A. F., and G. L. Mellor, A description of a three-dimensional coastal ocean model, in *Three-Dimensional Coastal Ocean Models, Coastal Estuarine Stud.*, vol. 4, edited by N. S. Heaps, pp. 1–16, AGU, Washington, D. C., 1987.

Brink, K. H., Coastal-trapped waves and wind-driven currents over the continental shelf, *Annu. Rev. Fluid Mech.*, *23*, 389–412, 1991.

Brink, K. H., Island-trapped waves, with application to observations off Bermuda, *Dyn. Atmos. Oceans*, *29*, 93–118, 1999.

Hogg, N. G., Observations of internal Kelvin waves trapped round Bermuda, *J. Phys. Oceanogr.*, *10*, 1353–1376, 1980.

Kantha, L. H., and C. A. Clayson, *Numerical Models of Oceans and Oceanic Processes*, 940 pp., Academic, San Diego, Calif., 2000.

Levitus, S., *NODC World Ocean Atlas 1994* [CD-ROM], Natl. Oceanic and Atmos. Admin., Silver Spring, 1994.

Longuet-Higgins, M. S., On the trapping of long-period waves round islands, *J. Fluid Mech.*, *37*, 773–784, 1969.

Longuet-Higgins, M. S., On the spectrum of sea level at Oahu, *J. Geophys. Res.*, *76*, 3517–3522, 1971.

Lumpkin, C. F., Resonant Coastal waves and superinertial oscillations, M. S. thesis, Dept. of Oceanogr., Univ. of Hawaii at Manoa, Honolulu, 1995.

Luther, D. S., Trapped waves around Hawaiian Islands, paper presented at 'Aha Huliko'a Hawaiian Winter Workshop, Univ. of Hawaii, Honolulu, 1985.

Mellor, G. L., T. Ezer, and L. Y. Oey, The pressure gradient conundrum of sigma coordinate ocean models, *J. Atmos. Oceanic Technol.*, *11*, 1126–1134, 1994.

Merrifield, M. A., P. E. Holloway, and T. M. S. Johnston, The generation of internal tides at the Hawaiian Ridge, *Geophys. Res. Lett.*, *28*, 559–562, 2001.

Miyata, M., and G. W. Groves, Note on sea level observations at two nearby stations, *J. Geophys. Res.*, *73*, 3965–3967, 1968.

Miyata, M., and G. W. Groves, A study of the effects of local and distant weather on sea level in Hawaii, *J. Phys. Oceanogr.*, *1*, 203–213, 1971.

Munk, W. H., and D. E. Cartwright, Tidal spectroscopy and prediction, *Philos. Trans. R. Soc., London, Ser. A*, *259*, 533–591, 1966.

Munk, W. H., and G. J. F. MacDonald, *The Rotation of the Earth*, 323 pp., Cambridge Univ. Press, New York, 1960.

Smith, W. H. F., and D. T. Sandwell, Global sea floor topography from satellite altimetry and ship depth soundings, *Science*, *277*, 1956–1962, 1997.

Wang, J.-J., H.-M. H. Juang, K. Kodama, S. Businger, Y.-L. Chen, and J. Partain, Application of the NCEP Regional Spectral Model to improve mesoscale weather forecasts in Hawaii, *Weather Forecasting*, *13*, 560–575, 1998.

Wunsch, C., The spectrum from two years to two minutes of temperature fluctuations in the main thermocline at Bermuda, *Deep Sea Res.*, *19*, 577–593, 1972.

D. S. Luther, M. A. Merrifield, and L. Yang, Department of Oceanography, University of Hawaii at Manoa, Honolulu, HI 96822, USA. (markm@soest.hawaii.edu)